Multichromophoric Cyclodextrins, Part 7

Photophysical and Structural Features of Inclusion Complexes with Fluorescent Dyes

Patricia Choppinet,[b, c] Ludovic Jullien,*[a] Bernard Valeur*[b, c]

Abstract: The synthesis of a new water-soluble β-cyclodextrin CD-St, with seven steroidic naphthalene chromophores linked to the primary rim, is reported together with the photophysical and structural features of its inclusion complexes with merocyanine and oxazine fluorescent dyes. These complexes were formed in a buffer at pH 10. At this pH the cyclodextrin is 14 times negatively charged since each chromophore bears two carboxylic groups. No excimer emission was detected, as expected from the design principles. Two complexes can be formed with stoichiometries 1:1 and 2:1 (CD:dye) for both dyes. The respective association constants were determined. In the 2:1 complexes, the cyclodextrin secondary rims are facing each other. Such complexes are outstanding artificial antennae with 14 chromophores surrounding an energy acceptor. Comparison was made with another (previously reported) water-soluble β-cyclodextrin CD-NA with seven naphthalene chromophores—also linked to the primary rim—but bearing only one carboxylic group each. In fact, CD-NA only forms 1:1 complexes with the same dyes. The difference in complexing ability of CD-NA and CD-St is discussed.

Keywords: cyanines · cyclodextrins · fluorescent dyes · inclusion compounds · merocyanine

Introduction

β-Cyclodextrin is a toroidal molecule containing seven glucopyranose units. Its cavity diameter is approximately 7 Å. Derivatives obtained by covalently linking seven chromophores to the primary or secondary rim exhibit very interesting features from various points of view.[1–10] The limited number of chromophores in well defined positions is a distinct advantage for the study of excitation energy transport[1, 5, 10] which is of major interest for the understanding of light collection in natural and artificial systems. Inclusion of an energy acceptor in the cavity leads to a supramolecular complex in which the antenna effect, that is energy transfer from the appended antenna chromophores to the encased acceptor, can be thoroughly studied.[4, 6] The circular arrangement of the antenna chromophores is reminiscent of the antenna system of photosynthetic bacteria[11] which further emphasizes the interest of multichromophoric cyclodextrins. Another outstanding feature is the capability of antenna-induced photoreactions within the cavity; specific effects are indeed expected from selective excitation of the reactants included in the cavity through energy transfer from the appended chromophores.[7, 8] Finally, multichromophoric cyclodextrins can be used as fluorescent sensors since the fluorescence emission is affected by complexation of an analyte; for instance, detection of very low concentrations of cationic surfactants has been recently reported by us.[9]

In our previous work devoted to the antenna effect in an inclusion complex of a water-soluble β-cyclodextrin CD-NA with a merocyanine (DCMOH) (Figure 1) we observed an excimer emission from the appended chromophores.[6] Later on, investigation of the complexation of several cationic surfactants[9] suggested that the excimer formation in CD-NA is likely to result from a head-to-tail interaction between two naphthalene units located on opposite sides of the functionalized primary rim. For a thorough study of the antenna effect, excimer formation should be avoided because excimers act as energy traps in the excitation energy hopping process, and energy transfer to an acceptor included in the cavity can occur from both monomer and excimer forms of the antenna chromophores. This precludes a detailed analysis of the dynamics of homotransfer (among antenna chromophores)

[a] Dr. L. Jullien
Département de Chimie (CNRS UMR 8640)
Ecole Normale Supérieure, 24, rue Lhomond
F-75231 Paris cedex 05 (France)
Fax: (+33) 1-44-32-33-25
E-mail: ludovic.jullien@ens.fr

[b] Prof. Dr. B. Valeur, Dipl.-Chem. P. Choppinet
Laboratoire PPSM (CNRS UMR 8531)
Département de Chimie, ENS-Cachan
61 Av. du Président Wilson, F-94235 Cachan cedex (France)

[c] Laboratoire de Chimie Générale
Conservatoire National des Arts et Métiers
292 rue St Martin, F-75141 Paris cedex 03 (France)

[±] Part 6: See ref. [10].

© WILEY-VCH Verlag GmbH, D-69451 Weinheim, 1999
0947-6539/99/0512-3666 $ 17.50+.50/0

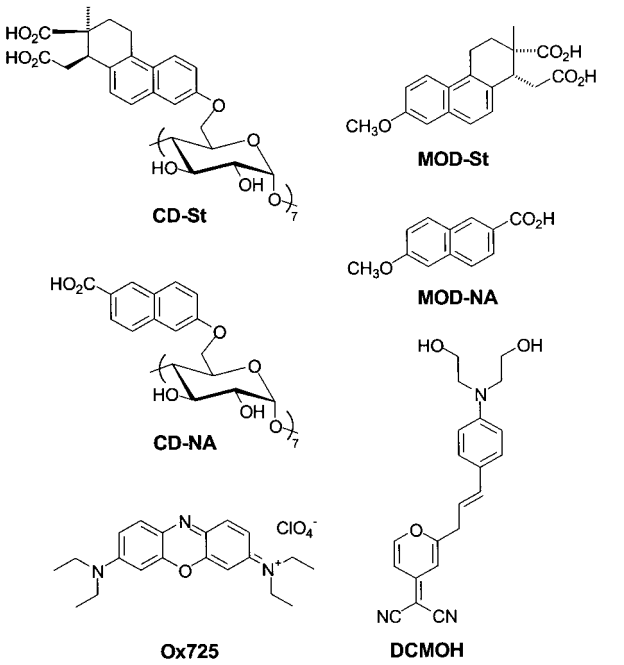

Figure 1. Molecular structure of the molecules CD-St, MOD-St, CD-NA, MOD-NA, DCMOH, Ox725.

andheterotransfer (from the antenna chromophores to an included acceptor).

In order to avoid excimer formation, we have designed a new water-soluble β-cyclodextrin according to the following principles. Additional repulsive interactions between the chromophores are introduced because such repulsions can increase the average interchromophore distance at equilibrium and delay excimer formation within the excited state lifetime of the chromophores. Thus we sought for individual chromophoric units that would be i) nonplanar to disfavor molecular stacking and ii) "locally" more charged than in CD-NA, for instance, containing more than one ionizable group. In view of the expected similarity of their spectral features to the previously investigated naphthalenic series, the steroid backbones, whose A and B cycles are aromatic, have been selected. Upon additional considerations of structure, synthetic access and strategy, the β-cyclodextrin-6^A,6^B,6^C,6^D,6^E,6^F,6^G-hepta-*O*-bis-dehydro-isomarrianolic acid, hereafter noted CD-St was eventually chosen as a target.

In the present work, the synthesis of CD-St is reported together with the photophysical and structural features of its inclusion complexes with a merocyanine dye (DCMOH) and an oxazine dye (Oxazine 725) (see Figure 1). In particular, special attention will be paid to the structure of these complexes since they turned out to be very different from the inclusion complex of DCMOH with CD-NA.[6] This investigation is a prerequisite to a detailed study of the dynamics of the antenna effect to be published later on.

Abstract in French: *Cet article présente la synthèse d'une β-cyclodextrine hydrosoluble, CD-St, portant sept chromophores naphtaléniques inclus dans un squelette stéroïde, ainsi que les propriétés structurales et photophysiques de ses complexes d'inclusion vis-à-vis de colorants fluorescents (mérocyanine et oxazine). En milieu tamponné à pH 10, CD-St, portant quatorze charges négatives, ne présente aucune émission attribuable à la formation d'excimères. CD-St forme des complexes de stoechiométrie CD:colorant 1:1 et 2:1 dont les constantes d'association ainsi que les structures ont été analysées. La stabilité des complexes est comparée aux résultats obtenus lors de l'étude antérieure de CD-NA, autre β-cyclodextrine heptachromophorique hydrosoluble, qui donnait des complexes de stoechiométrie 1:1. Les faces secondaires des unités CD-St sont accolées dans les complexes de stoechiométrie 2:1 qui forment ainsi de remarquables antennes artificielles avec leurs quatorze chromophores entourant un accepteur d'énergie.*

Results and Discussion

Synthesis of CD-St: The first part of the synthesis of CD-St is displayed in Scheme 1. It starts from the estron methylether **1** that is aromatized in a first step to provide the d-isoequilenin methylether (**2**). The latter is transformed into the bis-dehydro-isomarrianolic acid methylether (**3**) by iodine oxidation. The deprotection of **3** by boron tribromide afforded the bis-dehydro-isomarrianolic acid (**4**) which was then esterified by diazomethane to give the diester **5**. The two last steps are performed under the conditions that were used for the CD-NA synthesis[6] (Scheme 2): i) condensation of the phenol **5** on the per-2,3-*O*-acetyl-6-iodo-β-cyclodextrin[12] to yield the perfunctionalized derivative **6**; ii) final saponification[13] followed by acidification to give the β-cyclodextrin-6^A,6^B,6^C,6^D,6^E,6^F,6^G-hepta-*O*-bis-dehydro-isomarrianolic acid (**7**) or CD-St.

Photophysical properties of CD-St: The properties of CD-St are compared with those of the bis-dehydro-isomarrianolic acid methylether (**3**) that is noted MOD-St in Figure 1. In fact, the latter compound is a valuable reference for evaluating the behavior of a noninteracting chromophore and can thus be used for estimating the strength of coupling between the individual steroid units in CD-St.

In a multichromophoric molecule like CD-St whose intrinsic interchromophoric and intercharge distances lie in the range of the characteristic lengths for chromophore coupling and for charge–charge interaction (vide infra), the photophysical features are expected to strongly depend on the chromophore arrangement along the primary rim. Since CD-St is a polyacid, the possible significance of pH and ionic strength I on controlling the photophysical features was first investigated. As in the previous studies,[4, 6] Britton–Robinson buffers[14] containing the same buffering components over the whole range of pH at constant ionic strength were used for the present investigation.

Absorption spectra: Both CD-St and MOD-St molecules are soluble in aqueous solution beyond pH 6 at $I = 0.1$M. Figure 2 displays the absorption spectra of CD-St and of the corresponding model MOD-St in a buffer solution at pH 10 ($I = 0.1$M) and EtOH 95:5 (v/v). CD-St and MOD-St exhibit a similarly shaped absorption band in the 300–350 nm range.

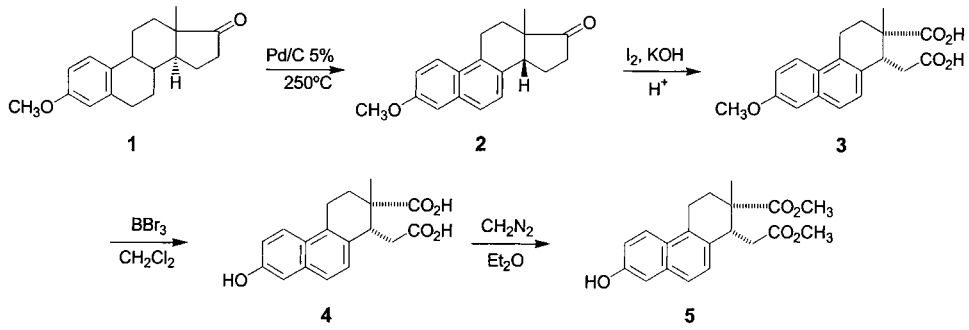

Scheme 1. Synthesis of compound **5**.

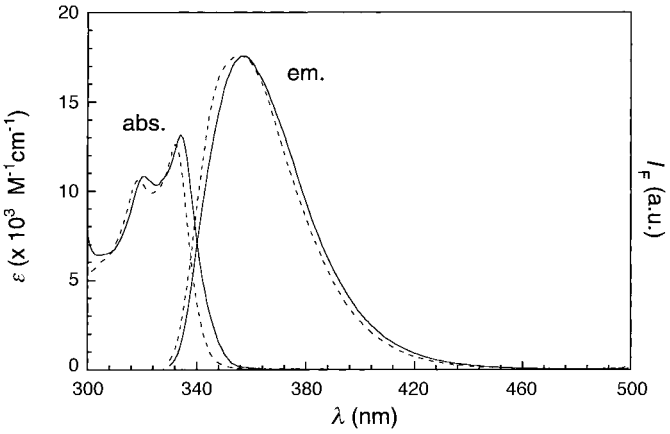

Figure 2. Absorption and corrected fluorescence spectra ($\lambda_{exc} = 320$ nm) of CD-St (straight line) and its corresponding model MOD-St (dotted line) in a mixture of buffer at pH 10 ($I = 0.1$M) and EtOH 95:5 (v/v). For comparison, the molar absorption coefficient of MOD-St has been multiplied by seven whereas both fluorescence spectra have been normalized at the same height at the maximum.

In contrast to CD-NA that exhibited a noticeable hypochromic effect with regard to its corresponding model MOD-NA, the molar absorption coefficients of CD-St and MOD-St are identical over the 300–350 nm range when they are normalized for seven chromophores. This result is in line with the smaller molar absorptivity of CD-St while keeping similar interchromophoric distance.[15]

The absorption spectrum of CD-St is not significantly affected by pH over the 5–10 pH range at $I = 0.1$M. The present result is in contrast to the previous CD-NA series. It can be accounted for by considering that i) the ionizable group was directly grafted on the aromatic chromophore in CD-NA but is not conjugated in CD-St and ii) the excitonic coupling between the individual chromophores is weaker in CD-St than in CD-NA (vide supra). Any pH-induced conformational change is thus expected to lead to smaller modifications of the absorption spectrum in CD-St. Similarly, the ionic strength does not significantly affect the CD-St spectrum at pH 10 in the 0.005–1M range. The difference of behavior with respect to CD-NA probably relies on the same explanation as for accounting for the pH effect.

Emission spectra: Figure 2 displays the emission spectra of CD-St and MOD-St in a mixture of buffer at pH 10 ($I = 0.1$M) and EtOH 95:5 (v/v) ($\lambda_{exc} = 320$ nm). The spectrum of both compounds consists of a band exhibiting a maximum at 353 nm. The absence of any shoulder or band broadening demonstrates that excimers are not formed in CD-St. This observation confirms the validity of the present approach aiming to hinder the interaction between the individual chromophores of CD-St and made the latter a good candidate for investigating the detailed kinetics of energy heterotransfer in photophysically active CD-St-guest complexes.

Above pH 6, the pH has no influence on the emission spectrum of CD-St whereas the emission intensity strongly drops at pH 5. The latter observation reveals the intra- or intermolecular chromophore aggregation that takes place when the extent of the deprotonation of CD-St is too low. In fact, at $I = 0.1$M, the inverse Debye length κ^{-1}, that is the characteristic distance for screening electrostatic interaction, is equal to 1.0 nm.[16] Since the intercharge distance between two neighboring chromophores is about 1 nm, it can be concluded that each individual steroid unit in CD-St behaves more or less independently regarding electrostatic interaction. Since the apparent pK_a at $I = 0.1$M of the two carboxylic acids in MOD-St should be about 5–6,[17] it appears reasonable to expect that an extensive ionization takes place from pH 6.[18] Similarly, the ionic strength of the solution has no influence on the emission spectra of CD-St at pH 10 in the range 0.005–1M.

In view of the smaller molar absorption coefficient of CD-St compared with CD-NA and its anticipated similar complexing capability, the experiments devoted to evidence and characterize association had to be made at larger concentrations of derivatized cyclodextrin. As a consequence, special attention was paid to the aggregation behavior that can

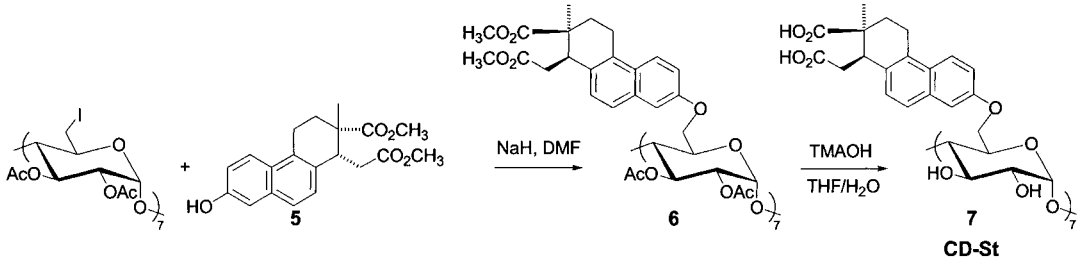

Scheme 2. Synthesis of CD-St (**7**).

© WILEY-VCH Verlag GmbH, D-69451 Weinheim, 1999
0947-6539/99/0512-3668 $ 17.50+.50/0 *Chem. Eur. J.* **1999**, *5*, No. 12

sometimes obscure the interpretation for deriving association constants.[19] In the present steroid series, this investigation is especially necessary since several steroids exhibit detergent properties (bile acids, etc.) and since its stereochemistry gives some facial[20] amphiphilic character to the bis-dehydro-isomarrianolic acid skeleton. In a first series of experiments, the Beer–Lambert law was checked for absorption of MOD-St and CD-St over the 0–150 μM and 0–15 μM, respectively concentration range in the 6–10 pH range at $I = 0.1$ M. Such results are only marginally informative for the present purpose since the comparison between the absorption features of MOD-St and CD-St suggested the absence of large modifications of the absorption spectra that should be consecutive to aggregation phenomena. The same experiments were repeated for the emission spectra since the quantum yield of fluorescence emission is generally a very sensitive probe towards aggregation. The absence of any deviation from the Beer–Lambert law for emission demonstrated that both MOD-St and CD-St molecules do not aggregate in the concentration range that was investigated in the absorption experiments. Furthermore, the absence of dependence of the excited-state lifetimes of MOD-St and CD-St (data not shown) as a function of their concentrations in a mixture of buffer at pH 10 ($I = 0.1$ M) and EtOH 95:5 (*v*/*v*) further support the absence of aggregation.

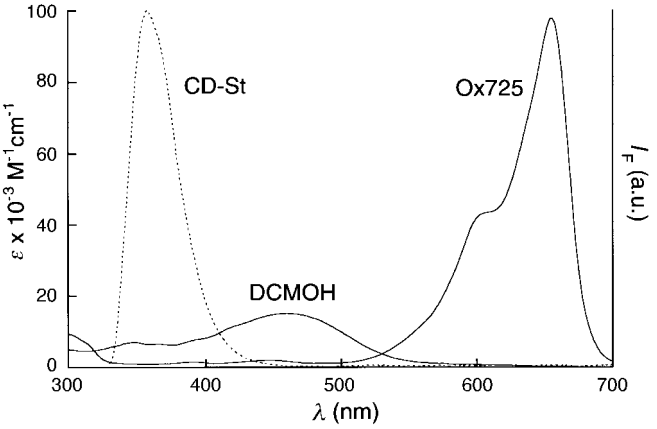

Figure 3. Corrected fluorescence spectrum of CD-St (dotted line) and absorption spectra of DCMOH and Ox725 (straight lines) in a mixture of buffer at pH 10 ($I = 0.1$ M) and EtOH 95:5 (*v*/*v*).

Photophysical features and self-association of the guest dyes: To examine the influence of the overlap of the acceptor absorption spectrum with the emission of CD-St, we look for two molecules fulfilling the previously reported constraints for complexation and photophysics[6] and that should additionally exhibit absorption maxima at very different wavelengths. The previously investigated DCMOH merocyanine was selected as the acceptor with a good spectral overlap whereas the red-absorbing Oxazine 725 (Ox725) was anticipated to be a poor acceptor[21] (Figure 1). Figure 3 displays the fluorescence spectrum of CD-St and the absorption spectra of DCMOH and Ox725 in a mixture of buffer at pH 10 ($I = 0.1$ M) and EtOH 95:5 (*v*/*v*). DCMOH and Ox725 exhibit their respective absorption maximum at 460 and 655 nm. The much smaller spectral overlap for Ox725 is clearly shown in Figure 3.

In view of the rather large concentrations that were anticipated to be required for extracting the association constants (vide supra), the possible aggregation of DCMOH and Ox725 at high concentrations was first investigated. Whereas Ox725 conforms to the Beer–Lambert law for absorption spectra in the 1–50 μM concentration range and for emission spectra in the 1–5 μM[22] concentration range, DCMOH exhibits a behavior that implies a dependency on its concentration. On increasing the latter, a small hyperchromism is observed within the 0.6–1.5 μM range and accompanied by a significant blue-shift of the absorption whereas the increase of fluorescence emission is dampered at large concentrations. Figure 4 quantitatively displays the role of the DCMOH concentration on the absorption at 460 nm (Figure 4, left) and the fluorescence emission at 630 nm ($\lambda_{exc} = 460$ nm; Figure 4, right). A

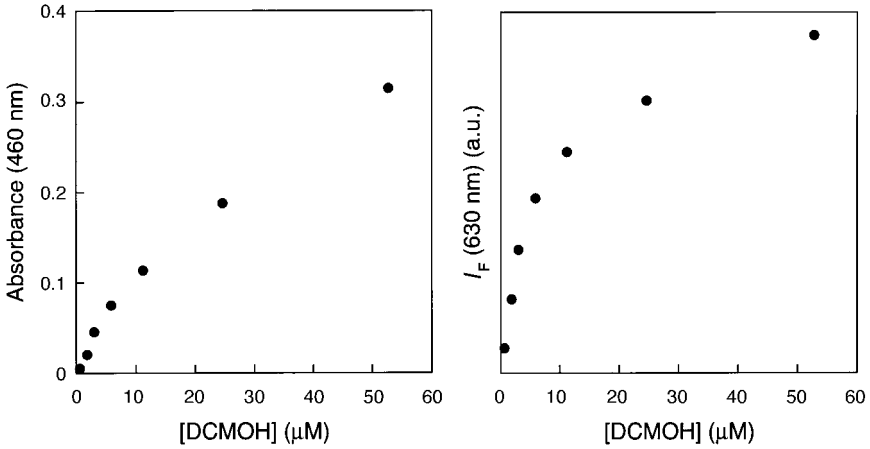

Figure 4. Absorption at 460 nm (left) and corrected fluorescence spectra at 630 nm ($\lambda_{exc} = 460$ nm) (right) of DCMOH as a function of the DCMOH concentration in a mixture of buffer at pH 10 ($I = 0.1$ M) and EtOH 95:5 (*v*/*v*).

single rather abrupt change of the absorption and fluorescence regime occurs at concentrations around 8 μM. In view of the limited water solubility of DCMOH, a two-step aggregation process has been envisaged to account for these observations. As a result of the large dipole moment of DCMOH, a head-to-tail dimerization is first expected at intermediate concentrations. The excitonic coupling within the corresponding species would indeed lead to the observed blue shift in absorption[23] and the DCMOH aggregation would be accompanied with a significant drop of its fluorescence quantum yield. At the largest concentrations, one should observe the formation of much larger aggregates that would not further affect the absorption while still leading to the decrease of fluorescence emission. The aggregation

phenomenon has been additionally evidenced by phase fluorimetry experiments at different DCMOH concentrations. Whereas the observed DCMOH fluorescence decay is a single exponential at 4.7 μM, a longer decay time appears at 41 μM (Table 1) which arises from the poorly fluorescent

Table 1. Decay times of DCMOH under different experimental conditions ($\lambda_{exc} = 442$ nm, $T = 298$ K).

Conditions	τ [ns]	f[a]	χ_r^2[b]
pH 10 buffer 4.7 μM	0.386 ± 0.006	1	0.852
pH 10 buffer 41 μM	0.387 ± 0.006	0.96	
	1.53 ± 0.24	0.04	1.592
pH 10 buffer with CD-St (8.2 μM)	0.61 ± 0.06	0.04	
([DCMOH]/[CD-St] = 0.5)	3.49 ± 0.04	0.96	0.934

[a] Fractional intensities. [b] Reduced chi-square.

DCMOH aggregates. The fluorescence emission data displayed in Figure 4, right, have been analyzed in the low concentration regime to extract the dimerization constant K_{dim} associated to the Equations:

$$2\,DCMOH = (DCMOH)_2 \quad (1)$$

The following equations:

$$I_f = \alpha_1[DCMOH] + \alpha_2[(DCMOH)_2] \quad (2a)$$

$$I_f = \left(\frac{2\alpha_1 - \alpha_2}{8K_{dim}}\right)\left(\sqrt{1 + 8K_{dim}[DCMOH]_{tot}} - 1\right) + \frac{\alpha_2}{2}[DCMOH]_{tot} \quad (2b)$$

are used for fitting the data where I_f denotes the fluorescence intensity, α_1 and α_2 are the proportionality factors, respectively, relating the fluorescence emission of DCMOH and $(DCMOH)_2$ to their concentrations, and $[DCMOH]_{tot}$ is the total concentration of dye in the solution.[24] A dimerization constant equal to $K_{dim} = 5.3 \times 10^5$ ($\log K_{dim} = 5.7$) (reference system: infinitely diluted solution parametered by molar concentrations) and $\alpha_2/\alpha_1 = 0.26$ are thus obtained. The self-aggregation of DCMOH is a severe limit for investigating the CD-St:DCMOH association since only rather low concentration ratios [DCMOH]/[CD-St] will be accessible for reasonably extracting the thermodynamic constants (vide infra).

First evidences for the CD-St:dyes interaction: The interaction between the CD-St host and the DCMOH and Ox725 guests can be revealed by observing either the host or the guest absorption and emission features.

CD-St:DCMOH interaction: To examine the possible modifications of the photophysical properties of the dye, a first series of experiments was performed at constant DCMOH concentration (6.0 μM). Upon addition of increasing amounts of CD-St, a red shift from 463 nm to 480 nm of the DCMOH charge transfer absorption band was observed (Figure 5, left). At the same time, the direct excitation of the DCMOH fluorescence emission ($\lambda_{exc} = 460$ nm) led to a large increase of emission intensity that was accompanied by a blue shift from 637 nm to 586 nm (Figure 5, right). The evolution of the fluorescence emission is first discussed. Indeed, since the fluorescence quantum yields of the DCMOH aggregates are much lower than that of the monomer, this evolution is essentially related to the monomer behavior. As a result of its larger dipole moment in the excited state, both increases of fluorescence emission and blue shift are in line with the transfer of the DCMOH from the aqueous solution to a less polar and less relaxed environment such as the cyclodextrin cavity.[6] According to the same reasoning, a blue shift would have been expected upon DCMOH interaction with CD-St in the absorption spectrum. However, the experimentally observed behavior has to be interpreted in the light of the above-mentioned aggregation study of DCMOH. Hence the red-shift is not governed by a change of polarity but it simply reflects the dissociation of the DCMOH aggregates (dimers at a DCMOH concentration equal to 6 μM) upon addition of CD-St.

CD-St:Ox725 interaction: A similar series of experiments was performed at constant Ox725 concentration (2.0 μM). Figure 6, left, shows that the absorption band of Ox725 is red-shifted and slightly decreased when CD-St is added. The latter observations point out the existence of a CD-St:Ox725 interaction. Nevertheless, they cannot be used for evaluating the environmental changes upon interaction since the symmetrical merocyanine structure of Ox725 forbids the presence of strong solvatochromic effects. The evolution of the fluorescence emission spectrum by direct excitation of Ox725 ($\lambda_{exc} = 600$ nm) is displayed in Figure 6, right. The interaction with CD-St is accompanied by the quenching of the Ox725 fluorescence. The latter observation is probably related to an electron transfer from the naphthalene rings of the steroid units to the excited state of Ox725. Together with the short range of electron transfer, the absence of any relay for the reducing electrons in CD-St suggests that, like

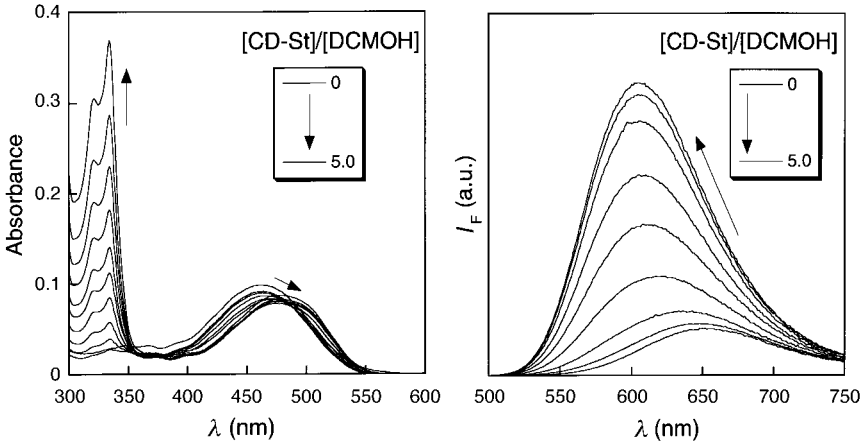

Figure 5. Absorption (left) and corrected fluorescence spectra ($\lambda_{exc} = 460$ nm) (right) of DCMOH as a function of the [CD-St]/[DCMOH] concentration ratio in a mixture of buffer at pH 10 ($I = 0.1$ M) and EtOH 95:5 (v/v). The DCMOH concentration is kept constant throughout the whole experiment at [DCMOH] = 6.0 μM.

© WILEY-VCH Verlag GmbH, D-69451 Weinheim, 1999
0947-6539/99/0512-3670 $ 17.50+.50/0 *Chem. Eur. J.* **1999**, *5*, No. 12

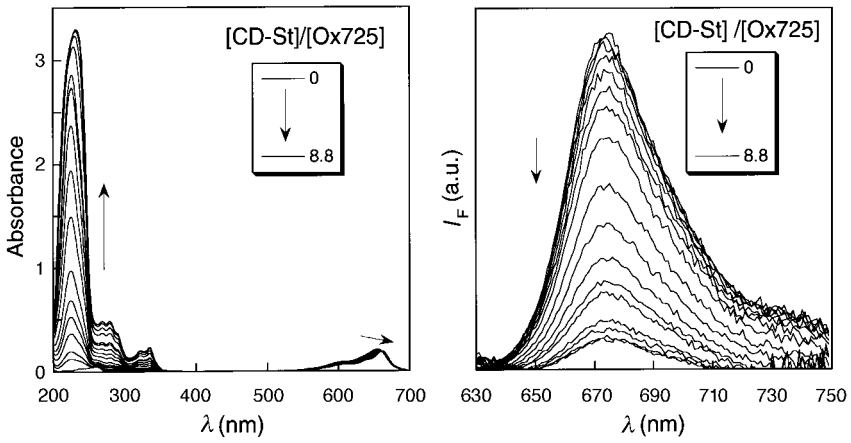

Figure 6. Absorption (left) and corrected fluorescence spectra ($\lambda_{exc} = 600$ nm) (right) of Ox725 as a function of the [CD-St]/[Ox725]concentration ratio in a mixture of buffer at pH 10 ($I = 0.1$M) and EtOH 95:5 (v/v). The Ox725 concentration is kept constant throughout the whole experiment at [Ox725] = 2.0 μM.

DCMOH, the Ox725 molecule is likely to be included within the CD-St cavity in the CD-St:Ox725 complex.

Antenna effect: Solutions of CD-St (9.3 μM for the DCMOH experiment and 6.8 μM for the Ox725 experiment) in a mixture of buffer at pH 10 ($I = 0.1$M) and EtOH 95:5 (v/v) at various concentrations of DCMOH or Ox725 were prepared. Figure 7, left, displays the evolution of the fluorescence emission of the solutions as a function of the [DCMOH]/[CD]-St ratio upon excitation at $\lambda_{exc} = 320$ nm. Upon increasing the DCMOH concentration, the fluorescence of the naphthalene chromophores decreases whereas the DCMOH fluorescence increases, even after correction of the contribution of the direct DCMOH excitation.[25] Under the same conditions, the addition of increasing amounts of DCMOH to a MOD-St solution does not induce any change of the emission signal of the naphthalene chromophore. The former observation provides evidence of the energy transfer from the excited naphthalenic antenna towards the included DCMOH. Figure 7, right, displays the evolution of the fluorescence emission of CD-St solutions when increasing amounts of Ox725 are added ($\lambda_{exc} = 320$ nm). As observed with DCMOH, the CD-St emission of fluorescence drops upon addition of Ox725. At the same time and although it is weak as a result of the low fluorescence quantum yield, the fluorescence emission of Ox725 gradually manifests. The present observation is in line with the energy transfer from the naphthalenic chromophores to the Ox725 guest. During this experiment, one can also notice that the Ox725 fluorescence becomes slightly red-shifted at the largest [Ox725]/[CD-St] ratios. This phenomenon is linked to the small Stokes shift of Ox725 and the consequent reabsorption of fluorescence which occurs when the absorbance becomes large enough at the wavelengths coresponding to the spectral overlap between the absorption and fluorescence spectra. A more detailed investigation of the kinetics of energy transfer process in relation with the absorption properties of the dye will be published elsewhere.

Characterization of the CD-St:dye complexes: The formation of inclusion complexes of DCMOH and Ox725 with CD-St was qualitatively evidenced by a first analysis of the series of experiments that have been presented in the last paragraph. In the next step, the thermodynamic characterization (stoichiometries and association constants) and the structural investigation of the CD-St:dye complexes are presented.

The stoichiometries of the associated species were first addressed by drawing Job's plots. The normalized deviation of the experimental data from the additive behavior that is expected without interaction is plotted as a function of the molar fractions at a constant sum of concentrations, that is [CD-St] + [dye]. The fluorescence emission provided the most sensitive signals for DCMOH. Figure 8, left, displays the results. Attention should be paid to the fact that the Job's plot was essentially recorded at DCMOH concentrations such that no DCMOH aggregation takes place so as not to possibly obscure the interpretation of the results. In the Ox725 case, the absorbance at 225 nm turned out to be a most sensitive indicator (Figure 8, right). For both dyes, a maximum of deviation is observed at a molar fraction of dye around ⅓ that points out a stoichiometry CD-St:dye equal to $2n:n$.[26] n can be deduced from the fine analysis of the Job's experiments with DCMOH. Indeed, one can notice that the two series of fluorescence experiments (λ_{exc}(CD-St) and λ_{em}(CD-St) or λ_{em}(dye); λ_{exc}(dye) and λ_{em}(dye)) address different

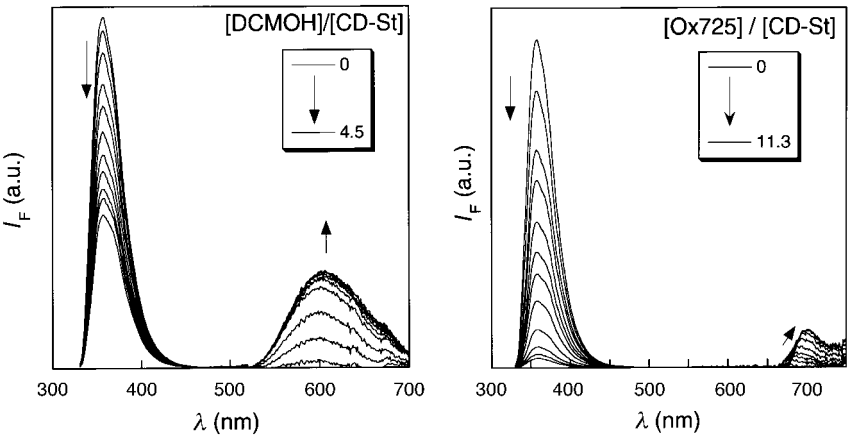

Figure 7. Evolution of the fluorescence spectra of CD-St solutions on addition of DCMOH for a concentration ratio [DCMOH]/[CD-St] = 0–4.5 (left) or Ox725 for a concentration ratio [Ox725]/[CD-St] = 0–11.3 (right). Solvent: buffer at pH 10 ($I = 0.1$M) and EtOH 95:5 (v/v). Excitation wavelength: $\lambda_{exc} = 320$ nm.

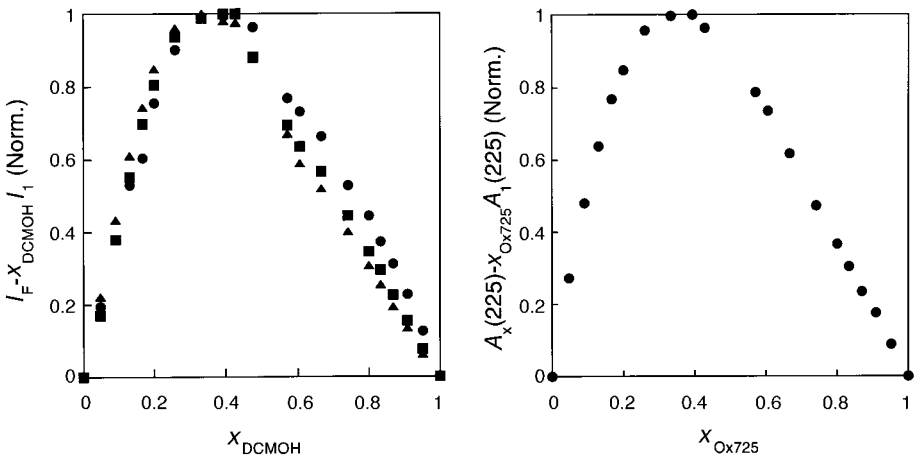

Figure 8. Job's plots. Left: variations of the normalized value of emission fluorescence ($I_F - x_{DCMOH}I_1$) at 358 nm ($\lambda_{exc} = 320$ nm, circles) and 585 nm ($\lambda_{exc} = 320$ nm, squares; $\lambda_{exc} = 460$ nm, triangles) as a function of $x_{DCMOH} =$ [DCMOH]/([DCMOH] + [CD-St]), at constant sum of concentrations ([DCMOH] + [CD-St] = 8.1 μM). I_1 is the fluorescence intensity for $x_{DCMOH} = 1$, i.e., without CD-St; right: variations of the normalized value of the absorbance at 225 nm [$A_x(225) - x_{Ox725}A_1(225)$] (circles) as a function of $x_{Ox725} =$ [Ox725]/([Ox725] + [CD-St]), at constant sum of concentrations ([Ox725] + [CD-St] = 10.9 μM). $A_1(225)$ is the absorbance for $x_{Ox725} = 1$, i.e., without CD-St. Solvent: buffer at pH 10 ($I = 0.1$M) and EtOH 95:5 (*v*/*v*).

ranges of interaction. Whereas the former series emphasizes a long range interaction linked with the process of energy transfer, the latter informs on the changes of the close environment of the dye. Hence, the complex stoichiometry remains unaffected by changing the spatial scale from a few angströms to a few nanometers, the latter distance being equal to the Förster radius (3.4 nm for DCMOH, 2.5 nm for Ox725; see Experimental Section). By considering the characteristic dimensions of the dye molecules and CD-St, the independence of the stoichiometry on the depth of probing interaction supports the sole presence of only one dye molecule in the close neighborhood of two CD-St molecules. The CD-St:dye stoichiometry is then 2:1.

For deriving the association constants β corresponding to the Equation (3):

$$2\,\text{CD-St} + \text{dye} = [(\text{CD-St})_2\text{:dye}] \quad (3)$$

we first simulated the experiments that were done for drawing Job's plots. The equilibrium and conservation laws were written for the experimental [CD-St] + [dye] total concentrations and the simulated normalized data were numerically calculated by solving the resulting polynomial equation for each values of the dye molar fraction. The best fit of the simulated to the experimental data yields the final β value. Both entries 1 of the Table 2 display the results for β so as the corresponding standard Gibbs free energies for Equation (3). The latter approach is not very precise for deriving β. In the present system, a more sensitive method for extracting β consists in processing the data that were obtained during the titration at constant dye concentration. A first nonlinear least-squares fit of the experimental data was attempted according to the general equation:

$$x = 2\left(\frac{I_F - I_0}{I_\infty - I_0}\right) + \frac{1}{[\text{dye}]_{tot}} - \left[\frac{1}{\beta}\left(\frac{I_F - I_0}{I_\infty - I_0}\right)^{1/2}\right] \quad (4)$$

where x is the ratio $[\text{CD-St}]_{tot}/[\text{dye}]_{tot}$, I_F is the fluorescence intensity for the considered x value, I_0 is the initial fluorescence intensity of the dye, I_∞ is the asymptotic intensity corresponding to the full complexation, $[\text{dye}]_{tot}$ is the total concentration in dye and β is the stability constant of the [$(\text{CD-St})_2$:dye] complex. In spite of a satisfactory fit, the plot of the residuals revealed some systematic deviation that led us to consider the successive complexation processes for both dyes:

$$\text{CD-St} + \text{dye} = [\text{CD-St:dye}] \quad (5a)$$

$$\text{CD-St} + [\text{CD-St:dye}] = [(\text{CD-St})_2\text{:dye}] \quad (5b)$$

with respective association constants K_{11} and K_{12} such as $\beta = K_{11}K_{12}$. To extract K_{11} and K_{12} and then β from the experimental data, a series of numerical simulations was performed by assuming that both associated species CD-St:dye and $(\text{CD-St})_2$:dye exhibit identical photophysical features (either molar absorption coefficients or quantum yields of fluorescence noted α in Table 2). As for Job's simulations, the equilibrium and conservation laws yielded a polynomial equation linking the simulated signal to

Table 2. Association constants β, corresponding Gibbs free energies $\Delta_r G^0_\beta$ and extrapolated parameters α describing the interactions between CD-St and the dyes DCMOH and Ox725 in a mixture of buffer at pH 10 ($I = 0.1$M) and EtOH 95:5 (*v*/*v*) at 298 K. The different entries correspond to the following experiments: 1) simulation of Job's plots; 2) titration of the dye at constant concentration by CD-St, see text.

Experiment	log β	$\Delta_r G^0_\beta$ [kJ mol^{-1}]	α
DCMOH			
1	11.5 ± 0.5[a]	-67 ± 4[a]	–[b]
2	11.5[c]	-67[c]	10.3[d]
	$\log K_{11} = 4$, $\log K_{12} = 7.5$		
Ox725			
1	11 ± 0.5	-63 ± 3	–[e]
2	10.7[f]	-61[b]	0.66[g]
	$\log K_{11} = 4$, $\log K_{12} = 6.7$		0.11[h]

[a] This value is an average over the treatment of the three different sets of experimental data that have been gathered under the following conditions: ($I_F - xI_1$) at 358 nm ($\lambda_{exc} = 320$ nm) or at 585 nm ($\lambda_{exc} = 320$ nm or $\lambda_{exc} = 460$ nm), see text. [b] Use was made of the value (10.3) extracted from experiment 2 to simulate Job's plot. [c] This value has been obtained by numerical simulation of the fluorescence emission of DCMOH at 610 nm ($\lambda_{exc} = 460$ nm) as a function of $x =$ [CD-St]/[DCMOH] at $[\text{DCMOH}]_{tot} = 6.0$ μM. In fact, K_{11} and K_{12} are obtained from the simulation and $\beta = K_{11}K_{12}$, see text. [d] Value extracted from fluorescence experiments. [e] Value (0.11) was extracted from experiment 2 (Ox725) to simulate Job's plot. [f] This value results from the averaging of the simulations of both the absorption at 600 nm and fluorescence emission at 670 nm ($\lambda_{exc} = 600$ nm) of Ox725 as a function of $x =$ [CD-St]/[Ox725] at $[\text{Ox725}]_{tot} = 2.0$ μM. In fact, K_{11} and K_{12} are obtained from the simulation and $\beta = K_{11}K_{12}$, see text. [g] From the simulation of the absorption at 600 nm. [h] From the simulation of the fluorescence emission at 670 nm ($\lambda_{exc} = 600$ nm).

© WILEY-VCH Verlag GmbH, D-69451 Weinheim, 1999
0947-6539/99/0512-3672 $ 17.50+.50/0 *Chem. Eur. J.* **1999**, *5*, No. 12

the ratio [CD-St]/[dye] at constant total concentration of the dye. The values of K_{11} and K_{12} that gave the best fit of the experimental data are given in both entries 2 of Table 2. The comparison of entries 1 and 2 is satisfactory. The association constants β corresponding to Equation (3) are rather large for a complexation in the β-cyclodextrin series. With regard to the previous CD-NA series, two points have to be underlined. First, the most favored association between the β-cyclodextrin and one dye molecule involves two CD molecules instead of one in the CD-NA system. Second, the association constant K_{11} is about ten times lower than the previously reported thermodynamic constant for the 1:1 complexation of DCMOH[6] or Ox725[27] by CD-NA.

Structural analysis of the (CD-St)$_2$:dye complexes: In view of the 2:1 stoichiometry of the CD-St:dye complexes, two axysymmetric arrangements for the associated species have been envisaged (Figure 9). Three different approaches were attempted to address the relative orientation of the cyclodextrin units in the complex.

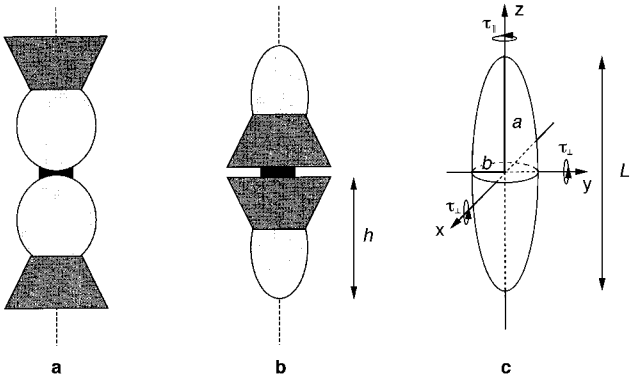

Figure 9. Possible relative arrangements of the CD-St and dye molecules in the (CD-St)$_2$:dye complexes (the averaged symmetry axis of two CD-St monomers are aligned and their **a**) primary or **b**) secondary rims are facing each other); **c**) modelization of the (CD-St)$_2$:DCMOH associated species as an axysymmetrical prolate ellipsoid, see text.

In a first series of experiments, the effect of ionic strength on the stability of the (CD-St)$_2$:dye complex was examined. Job's experiment for the system CD-St:DCMOH was repeated at an ionic strength equal to 5.10^{-3} M. Under such conditions, the Debye inverse length κ^{-1} is about 4 nm instead of about 1 nm at 0.1 M. As a result of the smaller distance between the interacting units in the (CD-St)$_2$:DCMOH complex when the cyclodextrin primary rims are facing (Figure 9a) than when the secondary faces are associated (Figure 9b) and in view of the κ^{-1} screened dependence of the electrostatic interaction, a more significant drop of the association constant is thus expected, when lowering the ionic strength, according to the scheme pictured in Figure 9a than in Figure 9b. In fact, both stoichiometry and association constant were found to be identical at the 0.1 M and 5.10^{-3} M values for the ionic strength. Although slightly surprising at first glance, such a result could be interpreted as disfavoring the association according to Figure 9a (vide infra).

In a second series of experiments, the addition of a guest specifically competing for the cyclodextrin cavity was envisaged. Indeed, whereas a major change of the extent for the process of dye complexation is expected if the dye is included within the cyclodextrin cavity, no dramatic change would occur if the dye simply interacts with the steroid walls according to Figure 9a. 1-Adamantane carboxylic acid (ADAC) was chosen as a specific competing inhibitor for the cyclodextrin cavity. Job's experiment was repeated for the couple CD-St:DCMOH in the presence of ADAC. With regard to the corresponding experiment without ADAC (see Figure 8), a broadening of the normalized signal as a function of the molar fraction of the dye was observed towards larger values. The present significant evolution points out the ADAC/DCMOH competition for complexation within the cavity. The Job's plot was numerically simulated as above by taking into account the chemical Equations (5a), (5b) and:

$$\text{CD-St} + \text{ADAC} = [\text{ADAC} \subset \text{CD-St}] \quad (6)$$

By using $\beta = 10^4 \times 10^{7.5}$ (See Table 2), the best fit of the experimental data led to a value equal to 10^4 for the association constant corresponding to Equation (6). In view of the possible contribution of an additional hydrophobic term, the latter value is in satisfactory agreement with already reported β-CD:ADAC association constants.[28] Consequently both the efficient role of ADAC as a competitor together with the quantitative agreement of the association constant support Figure 9b as the most probable for describing the CD-St:DCMOH interaction.

Eventually, a hydrodynamic approach was considered to complete the structural investigation. In fact, at low resolution, both structures displayed in Figures 9a and 9b can be envisioned as smooth bodies whose characteristic dimensions (length L and diameter D) are large enough with respect to the diameter of a water molecule so as to consider the surrounding aqueous medium as a continuum for analyzing the friction features. Under such conditions, the analysis of the hydrodynamic properties of a kinetically inert species such as the translational or rotational diffusion constants can be used to derive the molecular dimensions of the system.[29] In the present case, the rotational diffusion coefficient can be obtained from the analysis of the emission anisotropy. As a result of the intrinsic mobility of each steroid wall at room temperature and to the fast expected energy hopping between the individual chromophores along the CD-St primary rim, the observation of the CD-St emission anisotropy cannot be used for the present purpose. In contrast, the dye can be used as a probe for analyzing the motions of the whole complex. In fact, any rotation that should occur around an axis, that is perpendicular to the transition dipole moment during the lifetime of the excited state, is expected to affect the dye emission anisotropy. In the present investigation, it was impossible to apply this methodology to Ox725 since the fluorescence emission of the complexed Ox725 molecules is too weak for measuring their lifetime (vide supra). In contrast, the DCMOH is especially suited for the present analysis. The lifetimes τ and steady-state emission anisotropies $\bar{r}$ of DCMOH were measured in the presence of a large excess of CD-St. In the latter case, almost all DCMOH molecules are complexed so as to consider the corresponding

emission anisotropy to essentially result from the (CD-St)$_2$:DCMOH complex. The results are given in Table 1. Upon excitation at $\lambda_{exc} = 442$ nm, the fluorescence decay in the presence of CD-St is a double exponential with a short decay time corresponding to the lifetime of free DCMOH and a longer one corresponding to the lifetime in the CD-St complex; the former is indeed close to the lifetime measured in the absence of CD-St. The fact that the lifetime is much shorter in the buffer than in the cavity is consistent with the findings on fluorescence quantum yields: the ratio of lifetimes is 9.1, that is identical to the ratio of quantum yields (9.9). The steady-state emission anisotropies were then used for evaluating the molecular dimensions in the following manner. We first reasonably assumed that the (CD-St)$_2$:DCMOH association was tight with the main DCMOH axis aligned with the symmetry axis of the cyclodextrin dimer. In fact, such findings have been reported in the CD-NA series.[30] Moreover the DCMOH length and diameter fit both well with the internal volume of a β-cyclodextrin dimer. Second, the (CD-St)$_2$:DCMOH associated species was described as an axysymmetrical prolate ellipsoid (length L; diameter $\varnothing$; see Figure 9c). Under these conditions and by additionally considering that the transition dipole moment of DCMOH is oriented along the main molecular axis, the decay of emission anisotropy is a single exponential:[31]

$$r(t) = r_0 \exp(-6 D_\perp t) \tag{7}$$

where r_0 is the fundamental anisotropy and $D_\perp$ is the diffusion coefficient for rotation about an inertial axis perpendicular to the symmetry axis. The steady-state anisotropy can then be written as:

$$\frac{1}{\bar{r}} = \frac{1}{r_0}(1 + 6 D_\perp \tau) \tag{8}$$

where τ is the lifetime of the excited state.

The diffusion coefficient $D_\perp$ can be calculated by means of Perrin's equations for prolate symmetric ellipsoid:[32]

$$D_\perp = \frac{3\rho\{(2\rho^2-1)(\rho^2-1)^{-1/2}\ln[\rho + (\rho^2-1)^{1/2}] - \rho\}}{2(\rho^4-1)} D \tag{9}$$

where ρ is the axial ratio (i.e., ratio of the longitudinal semiaxis a to the equatorial semiaxis b of the ellipsoid) and $D = kT/6V\eta$ is the diffusion coefficient calculated for a sphere of the same volume and under the same conditions of temperature T and viscosity η. Stick boundary conditions are assumed to be valid.

The fundamental emission anisotropy r_0 of DCMOH was shown to be equal to 0.390 in a previous report.[6] The value of the steady-state emission anisotropy measured in the presence of an excess of CD-St ($\bar{r} = 0.146$), together with the excited-state lifetime of DCMOH in the cavity ($\tau = 3.49$ ns) are used to calculate the rotational diffusion coefficient $D_\perp$ of DCMOH (by means of Equation (8)). Then, Equation (9) allows us to derive a reasonable estimate of the axial ratio ($\rho = a/b = 1.75$) by taking $\eta = 10^{-3}$ Pa s^{-1} (water viscosity at room temperature). Moreover, the hydrodynamic diameter $\varnothing$ ($= 2b$) of CD-St can be evaluated to 2 nm by analogy with hydrodynamic measurements that have been performed on other β-cyclodextrin derivatives.[33] Therefore, the length of the ellipsoid $L = 2a$ is found to be 3.5 nm. The obtained L value compares well to the Quanta molecular model of the complex as in Figure 9b since the height of one CD-St molecule was evaluated to 1.7 nm.

In view of the results obtained along the different series of experiments that were performed for analyzing the fine structure of the (CD-St)$_2$:DCMOH complex, it thus appears more convincing to consider that the CD-St units self-assemble around the DCMOH by their secondary faces as pictured in Figure 9b than by their primary faces as displayed in Figure 9a.

Comparison of the complexing ability of CD-St and CD-NA towards DCMOH and Ox725: It is rather amazing that such similar compounds as the previously investigated CD-NA and the present CD-St do not lead to the same stoichiometry of the complexes with DCMOH and Ox725 dye molecules. Whereas 2:1 (CD:dye) complexes are formed with CD-St, only 1:1 associated species are obtained with CD-NA. Moreover, it is disturbing to observe that the dimerization occurs with the cyclodextrin derivative that bears the largest number of negative charges.

To understand this apparent paradox, we first evaluated the anticipated electrostatic interaction between two identically charged CD-NA molecules in the configuration presented in Figure 9b. According to the method that was already reported,[34] CD-NA was modeled as an heptagonal distribution of regularly spaced negative charges interacting in the frame of the Debye–Hückel theory. The electrostatic work that was associated to the process of building the dimer from two infinitely spaced CD-NA monomers was then evaluated to lie in the 15 and 30 kJ mol^{-1} range for an ionic strength equal to 0.1 M and 5×10^{-3} M, respectively.[35] From the present calculation and if only considering the (probably dominating) electrostatic term for CD–CD interaction, one should thus expect that: i) the stability of (CD-NA)$_2$:DCMOH is larger than that of (CD-St)$_2$:DCMOH. Indeed, at the same pH 10, CD-St bears about twice more negative charges than CD-NA so as to increase by a factor of 4 the corresponding electrostatic work for association;[34] and ii) the stability of the (CD-St)$_2$:DCMOH complex is markedly affected by lowering the ionic strength. Hence, the electrostatic work for association increases by a factor of 2 when going from 0.1 M to 5.10^{-3} M for the ionic strength.

The experimental observations contradict both preceding anticipations. In fact, the latter results are best explained in the frame of the nonlinear electrostatic screening that occurs when strongly charged bodies interact at rather low ionic strength. Some recent works emphasized the variety of regimes for electrostatic interaction that are observed when one overcomes the limits of applicability of the Debye-Hückel theory.[36] In fact, under the present conditions of concentration of supporting salt, a polyelectrolyte character most probably appears for CD-St whereas it is absent for CD-NA.[37] As a consequence, a significant part of the CD-St counterions should "collapse" on CD-St so as to considerably decrease its apparent charge for evaluating electrostatic interaction at a range beyond about a few angström. In the

 © WILEY-VCH Verlag GmbH, D-69451 Weinheim, 1999 0947-6539/99/0512-3674 $ 17.50+.50/0 *Chem. Eur. J.* **1999**, *5*, No. 12

CD-NA case, if no counterion condensation takes place, the seven charges of each CD-NA units will have to be taken into account for evaluating electrostatic interaction, whatever the considered range. Thus, even if CD-St is intrinsically (locally) more charged at very short range (0.1 nm), it could dimerize more easily than CD-NA since the dimerization process involves a repulsive electrostatic interaction at rather long range (about 3 nm according to Figure 9b). The theoretical evaluation of the proportion of counterions that are condensed on CD-St is difficult since it is expected to depend on the surface charge and the curvature of the molecule.[36] The present experimental results suggest that this proportion overcomes 0.5 since i) CD-St dimerizes in the presence of DCMOH whereas CD-NA does not, and ii) the same linear screening for electrostatic interaction will apply for both CD-St and CD-NA after correction of the condensed counterions. Under these conditions, the absence of any significant influence of the ionic strength on the stability of the $(CD\text{-}St)_2$:DCMOH complex cannot be easily explained in view of the possible changes of regimes for electrostatic interaction that can occur when the inverse Debye length drops below the local molecular curvature.[36]

Another way to approach the difference of behavior consists in comparing K_{11}(CD-St) with the association constant K(CD-NA) for the same dye substrates. In fact, one has $K(\text{CD-NA}) \approx 10 \times K_{11}(\text{CD-St})$. This means that the driving force for association is larger for CD-NA. One possible explanation should be that the molecular stacking is better at the level of the circular assembly of chromophores in CD-St than in CD-NA (less repulsive interaction between individual walls upon counterion condensation and possible better fit to the steric requirements for CD-St). Under such an assumption, the dye would be probably less deeply incorporated in the CD cavity in CD-St thus leading to a smaller 1:1 association constant K_{11}. Indeed the K_{12}(CD-St) value also supports this explanation in relation with a previous work where the dimerization constant K_{dim} of neutral cyclodextrins in water was obtained from extrapolation of the association constants for a series of oppositely charged cyclodextrin derivatives.[34] One has typically $K_{12}(\text{CD-St})/K_{11}(\text{CD-St}) \approx$ a few 10^3 whereas $K_{dim} \approx 1.5 \times 10^2$. Both processes involving cyclodextrin dimerization, the relation $K_{12}(\text{CD-St})/K_{11}(\text{CD-St}) > K_{dim}$ may point out the larger exposure of the hydrophobic dye within the CD-St cavity in the 1:1 complex.

Conclusion

In the present work, we have shown that CD-St can form complexes with DCMOH and Ox725 dyes and that the stoichiometries of these complexes are 1:1 and 2:1 (CD:dye). The respective association constants were found to be similar for both dyes. The absence of significant effect of the ionic strength and competition experiments led us to suggest that the cyclodextrin secondary rims are facing in the 2:1 complex. The fluorescence polarization data are consistent with a model of prolate ellipsoid. Comparison was made with CD-NA in which the seven naphthalene chromophores—also linked to the primary rim—bear only one carboxylic group each. CD-NA forms only 1:1 complexes with the same dyes. The difference with CD-St can be explained by the more pronounced polyelectrolyte character of CD-St in which the chromophores are likely to be more closely packed as a result of the collapse of a significant part of the counterions. The consequent decrease of the apparent charge to be considered in the electrostatic interaction can explain the absence of noticeable effect of ionic strength. Moreover, it is expected from this model that the dye is less deeply inserted in the CD cavity, which is consistent with the observation of a smaller K_{11} association constant for CD-St than for CD-NA.

In contrast to CD-NA, no excimer emission from CD-St was detected, as expected from the design principles. Therefore, the absence of excimers as energy traps is a distinct advantage for the study of the antenna effect. These 2:1 supramolecular complexes are indeed outstanding artificial antennae with 14 chromophores surrounding an energy acceptor. The antenna effect in these complexes, and in particular the dynamics of energy transfer, will the subject of a forthcoming paper.

Experimental Section

Synthesis: *General procedures*: Microanalyses were performed by the Service Central d'Analyse du CNRS (Vernaison) or by the Service de Microanalyses de l'Université Pierre et Marie Curie (Paris). Melting points were determined on a Kofler Heizbank. ^{1}H and ^{13}C NMR spectra were recorded in $CDCl_3$ at room temperature on a AM200 SY Bruker spectrometer operating at 200.13 MHz for ^{1}H and 50.3 MHz for ^{13}C; chemical shifts are reported in ppm with protonated solvent as internal reference (^{1}H: $CHCl_3$ in $CDCl_3$ $\delta = 7.26$, CHD_2COCD_3 in CD_3COCD_3 $\delta = 2.04$, CHD_2OD in CD_3OD $\delta = 3.30$, $CHDCl_2$ in CD_2Cl_2 $\delta = 5.32$; ^{13}C: $^{13}CDCl_3$ in $CDCl_3$ $\delta = 76.9$, $^{13}CD_3COCD_3$ in CD_3COCD_3 $\delta = 29.8$, $^{13}CD_3OD$ in CD_3OD $\delta = 49.0$, $^{13}CD_2Cl_2$ in CD_2Cl_2 $\delta = 53.8$); coupling constants J are given in Hz; homodecoupling and 2D carbon–proton correlations were used when necessary, to assign ^{1}H and ^{13}C NMR spectra (CD has been numbered from 1 to 6 and the steroid backbone from 1′ to 18′ in the usual way). C_{IV} and C_H stand for quaternary or hydrogen-bearing carbon atoms belonging to aromatic rings, respectively. Mass spectra (FAB positive) were performed by the Service de Spectrometrie de Masse du CNRS (Vernaison) and by Dr. Laprevote (ICSN CNRS, Gif sur Yvette). Column chromatography was performed on Merck silica gel 60 (0.040–0.063 mm). Analytical or preparative thin-layer chromatography (TLC) was conducted on Merck silica gel 60 F_{254} glass precoated plates. Visualization was accomplished with ultraviolet light, iodine, or sulfuric acid (5% in H_2O). Anhydrous solvents were purchased from SDS, France and used without further purification. β-Cyclodextrin from Orsan, France was dehydrated before use. Other commercially available reagents were used as obtained.

d-Isoequilenin methylether (**2**):[38] Estron methylether **1** (5.00 g, 18 mmol) and 5% palladium on charcoal were thoroughly mixed in a 50 mL two-necked flask fitted with a mechanical stirrer and an argon inlet tube. The flask was heated in a metal bath at 250–260 °C under constant flushing of argon while stirring from time to time. After cooling to room temperature, the mixture was thoroughly extracted with CH_2Cl_2 and filtered. The solvent was evaporated and the crude residue (4.60 g) was recrystallized from methanol to give **2** as a white powder (3.55 g, 70%): m.p. 118–120 °C (lit. 119–120 °C[38]); TLC (CH_2Cl_2): $R_f = 0.5$; ^{1}H NMR ($CDCl_3$): $\delta = 7.88$ (d, $J =$ 9.1 Hz, 1H, 4′), 7.62 (d, $J = 8.4$ Hz, 1H, 7′ or 8′), 7.28 (d, $J = 8.4$ Hz, 1H, 7′ or 8′), 7.20 (m, 2H), 3.93 (s, 3H, OCH_3), 3.1 (m, 3H), 2.4 (m, 3H), 1.9 (m, 2H), 1.7 (m, 1H), 1.16 (s, 3H, 18′); ^{13}C NMR ($CDCl_3$): $\delta = 204.0$ (17′), 157.1 (2′), 133.3 (C_{IV}), 132.45 (C_{IV}), 129.8 (C_{IV}), 127.8 (C_H), 127.3 (C_{IV}), 125.5 (C_H), 124.5 (C_H), 118.1 (C_H), 106.8 (C_H), 55.2 (OCH_3), 47.5 (14′), 46.75 (13′), 36.8, 28.9, 26.4, 21.8, 19.9 (18′).

Bis-dehydro-isomarrianolic acid methylether (**3**): A solution of I_2 (9.00 g, 35 mmol) in MeOH (120 mL) and a solution of KOH (16.74 g, 298 mmol) in water (30 mL) and MeOH (90 mL) were simultaneously added over 90 min to a well-stirred suspension of **2** (3.72 g, 13.3 mmol) in MeOH (370 mL). During addition, iodine was always present in excess. After partial evaporation of the solvent, a solution of KOH (6.00 g, 107 mmol) in water (40 mL) and MeOH (20 mL) was added and the mixture was refluxed for 1 h. After addition of activated charcoal and reflux for a few minutes, the suspension was filtered and cooled. The aqueous solution was extracted with ether and then acidified with concentrated hydrochloric acid. The acidic solution was extracted with ether. The organic phase was washed with water and dried over anhydrous sodium sulfate. Ether was then evaporated until deposition of the first crystals. After cooling, a pale-yellow precipitate of **3** was collected on a Büchner funnel (2.40 g, 55%): m.p. 245 °C (after recrystallization from ethyl acetate); ^{1}H NMR (CD_3COCD_3): $\delta = 10.75$ (br s, 2H), 7.94 (d, $J = 9.2$ Hz, 1H, 4′), 7.58 (d, $J = 8.5$ Hz, 1H, 7′ or 8′), 7.35 (d, $J = 8.5$ Hz, 1H, 7′ or 8′), 7.24 (d, $J = 2.6$ Hz, 1H, 1′), 7.17 (dd, $J = 2.6$, 9.2 Hz, 1H, 3′), 3.90 (s, 3H, OCH_3), 3.58 (dd, $J = 3.5$, 8.5 Hz, 1H, 14′), 3.29 (ddd, $J = 1.7$, 7.0, 18.0 Hz, 1H, 11′a), 3.01 (ddd, $J = 7.9$, 10.4, 18.0 Hz, 1H, 11′b), 2.61 (dd, $J = 3.5$, 15.8 Hz, 1H, 15′a), 2.38 (dd, $J = 8.5$, 15.8 Hz, 1H, 15′b), 2.20 (m, 2H, 12′), 1.21 (s, 3H, 18′); ^{13}C NMR (CD_3COCD_3): $\delta = 178.2$ (16′ or 17′), 173.6 (16′ or 17′), 158.0 (2′), 135.05 (C_{IV}), 134.55 (C_{IV}), 129.8 (C_{IV}), 129.55 (C_H), 128.55 (C_{IV}), 126.2 (C_H), 125.5 (C_H), 118.95 (C_H), 107.7 (C_H), 55.6 (OCH_3), 45.15 (14′), 43.9, 41.2, 26.4, 23.1, 22.55; anal. calcd for $C_{19}H_{20}O_5$: C 69.44, H 6.09; found: C 69.37, H 6.17.

Bis-dehydro-isomarrianolic acid (**4**): Boron tribromide (4 mL, 42 mmol) was slowly added with a syringe at −78 °C to a suspension of **3** (4.00 g, 12.8 mmol) in anhydrous CH_2Cl_2 (200 mL). The mixture was allowed to warm and was stirred for 2 h at room temperature. After addition of crushed ice, the biphasic mixture was made alkaline by addition of 1M NaOH[39] and the aqueous phase was separated. The fine precipitate remaining suspended in CH_2Cl_2 was extracted several times with 1M NaOH. The different alkaline fractions were collected and acidified with concentrated hydrochloric acid. After filtration, the precipitate was washed with water to yield **4** as a yellowish powder (3.65 g, 95%): m.p. 226–228 °C (after recrystallization from benzene); ^{1}H NMR (CD_3OD): $\delta = 7.84$ (d, $J = 8.8$ Hz, 1H, 4′), 7.41 (d, $J = 8.6$ Hz, 1H, 7′ or 8′), 7.21 (d, $J = 8.6$ Hz, 1H, 7′ or 8′), 7.07 (dd, $J = 2.6$, 8.8 Hz, 1H, 3′), 7.04 (d, $J = 2.6$ Hz, 1H, 1′), 3.52 (dd, $J = 2.8$, 8.4 Hz, 1H, 14′), 3.27 (dd, $J = 5.7$, 10.9 Hz, 1H, 11′a), 3.00 (m, 1H, 11′b), 2.58 (dd, $J = 3.7$, 15.4 Hz, 1H, 15′a), 2.35 (dd, $J = 8.5$, 15.4 Hz, 1H, 15′b), 2.1 (m, 2H, 12′), 1.21 (s, 3H, 18′); ^{13}C NMR (CD_3OD): $\delta = 180.65$ (16′ or 17′), 176.2 (16′ or 17′), 155.85 (2′), 135.55 (C_{IV}), 133.8 (C_{IV}), 129.5 (C_H), 129.3 (C_{IV}), 128.2 (C_{IV}), 126.1 (C_H), 125.6 (C_H), 118.9 (C_H), 110.8 (C_H), 45.6 (14′), 44.4, 42.0, 26.55, 23.35, 22.6; anal. calcd for $C_{18}H_{18}O_5 \cdot \frac{1}{3}C_6H_6$: C 67.40, H 5.66; found: C 67.48, H 5.73; anal. calcd for $C_{18}H_{18}O_5$ (the sample was dried under vacuum at 160 °C for 48 h): C 68.79, H 5.73; found: C 68.64, H 5.86.

Bis-dehydro-isomarrianolic acid dimethylester (**5**): A solution of diazomethane (5 mL) in diethyl ether was slowly added to a suspension of **4** (1.00 g, 3.2 mmol) in ether (5 mL) at 0 °C. After the solution was stirred for 10 min at 0 °C, the solvent was evaporated. The residue was dissolved in MeOH and treated with activated charcoal Norit A. After filtration and evaporation of the solvent, the resulting oil was purified by chromatography (silica gel hexane/ethyl acetate 2:1) to yield **5** as a glassy solid (1.00 g, 92%). This solid is easier to handle after dissolution in a minimum of ether and evaporation under high a vacuum. This compound is fairly unstable and has to be chromatographed before use: TLC (cyclohexane/ethyl acetate 7:3): $R_f = 0.4$; ^{1}H NMR ($CDCl_3$): $\delta = 7.80$ (d, $J = 9.8$ Hz, 1H, 4′), 7.44 (d, $J = 8.6$ Hz, 1H, 7′ or 8′), 7.17 (d, $J = 8.6$ Hz, 1H, 7′ or 8′), 7.12 (dd, $J = 2.4$, 7.8 Hz, 1H, 3′), 7.11 (s, 1H, 1′), 6.77 (s, 1H, OH), 3.76 (s, 3H, OCH_3), 3.67 (s, 3H, OCH_3), 3.61 (dd, $J = 5$, 6 Hz, 1H, 14′), 3.28 (dd, $J = 6$, 17.5 Hz, 1H, 11′a), 2.97 (ddd, $J = 8$, 10.5, 18 Hz, 1H, 11′b), 2.57 (dd, $J = 5$, 15 Hz, 1H, 15′a), 2.46 (dd, $J = 7.5$, 17.5 Hz, 1H, 15′b), 2.31–2.03 (m, 2H, 12′), 1.24 (s, 3H, 18′); ^{13}C NMR ($CDCl_3$): $\delta = 177.5$ (16′ or 17′), 173.1 (16′ or 17′), 153.4 (2′), 133.8 (C_{IV}), 132.4 (C_{IV}), 128.7 (C_{IV}), 128.4 (C_H), 127.1 (C_{IV}), 125.2 (C_H), 124.7 (C_H), 117.6 (C_H), 110.2 (C_H), 51.8 (OCH_3), 51.6 (OCH_3), 44.5 (14′), 43.3, 40.8, 25.05, 22.1, 21.7; anal. calcd for $C_{20}H_{22}O_5 \cdot 0.4\,H_2O$: C 68.75, H 6.57; found: C 69.07, H 6.82.

*2^A,2^B,2^C,2^D,2^E,2^F,2^G,3^A,3^B,3^C,3^D,3^E,3^F,3^G-Tetradeca-*O*-acetyl-β-cyclodextrin-6-^{A},6^B,6^C,6^D,6^E,6^F,6^G-hepta-*O*-bis-dehydro-isomarrianolate dimethylester* (**6**): A suspension of **5** (250 mg, 0.73 mmol) and 80% NaH (21 mg, 0.73 mmol) in dry DMF (5 mL) is stirred under argon for 50 min at room temperature. Per-2,3-*O*-acetyl-6-iodo-β-cyclodextrin (100 mg, 0.041 mmol) is then added and the mixture is further stirred for 100 min at room temperature. After addition of water, the aqueous phase is extracted with ethyl acetate. The organic phase is extensively washed with water and dried over sodium sulfate. After solvent evaporation, the crude residue (340 mg) is purified (first column: silica gel hexane/ethyl acetate 2:1; second column: silica gel chloroform/methanol 97.5:2.5). The appropriate fractions (140 mg) are purified by TLC (1 mm silica gel plates; chloroform/hexane/1-butanol 50:70:15). After trituration in methanol, **6** was obtained as a white powder (40 mg, 25%): TLC (hexane/ethyl acetate/butanol 5:5:1.5): $R_f = 0.6$; FAB-MS calcd $[M+H]^+$ 3995.0, found 3994.7; ^{1}H NMR (CD_2Cl_2): $\delta = 7.62$ (d, $J = 9.2$ Hz, 1H, 4′), 7.10 (dd, $J = 2.2$, 9.2 Hz, 1H, 3′), 7.03 (d, $J = 8.8$ Hz, 1H, 7′ or 8′), 7.01 (d, $J = 8.8$ Hz, 1H, 7′ or 8′), 6.79 (d, $J = 2.2$ Hz, 1H, 1′), 5.52 (dd, $J = 8.5$, 9.7 Hz, 1H, 3), 5.13 (d, $J = 3.6$ Hz, 1H, 1), 4.82 (dd, $J = 3.6$, 9.7 Hz, 1H, 2), 4.39 (m, 2H, 5, 6a), 4.08 (m, 2H, 4, 6b), 3.67 (s, 3H, OCH_3), 3.63 (s, 3H, OCH_3), 3.5 (m, 1H, 14′), 2.9 (m, 1H, 11′a), 2.6 (m, 1H, 11′b), 2.44 (dd, $J = 5$, 16 Hz, 1H, 15′a), 2.34 (dd, $J = 7$, 16 Hz, 1H, 15′b), 2.0–1.7 (m, 2H, 12′), 2.15 (s, 3H, $COCH_3$), 2.10 (s, 3H, $COCH_3$), 1.03 (s, 3H, 18′); ^{13}C NMR (CD_2Cl_2): $\delta = 177.3$ (17′), 172.9 (16′), 170.9 (CO-3), 170.1 (CO-2), 156.1 (2′), 134.3 (6′), 133.9 (9′), 129.5 (7′), 129.5 (5′), 128.0 (10′), 126.1 (8′), 125.6 (4′), 117.6 (3′), 108.9 (1′), 97.4 (1), 76.8 (4), 71.6 (3), 71.2 (2, 5), 67.5 (6), 52.0 (17′-OCH_3), 51.9 (16′-OCH_3), 44.8 (13′), 43.7 (14′), 41.2 (15′), 25.6 (11′), 22.6 (12′), 22.1 (18′), 21.2 (3-CH_3), 21.1 (2-CH_3).

*β-Cyclodextrin-6^A,6^B,6^C,6^D,6^E,6^F,6^G-hepta-*O*-bis-dehydro-isomarrianolic acid* (**7**): A biphasic mixture of **6** (25 mg, 0.0063 mmol) in THF (0.5 mL) and tetramethylammonium hydroxide (319 mg, 1.76 mmol) in water (0.5 mL) was vigorously stirred for 3 h 30 min at 65 °C. After cooling, water (1 mL) was added and the mixture was extracted with ethyl acetate. The aqueous phase was acidified with AcOH. The resulting suspension was centrifugated and the precipitate was extensively washed with water. After drying under vacuum, **7** was obtained as a white powder (21 mg, quantitative): FAB-MS calcd $[M+Li]^+$ 3216, found 3218; ^{1}H NMR ($[D_6]$DMSO + εTFA (trifluoroacetic acid)): $\delta = 7.10$ (d, $J = 9.0$ Hz, 1H), 6.95 (m, 3H), 6.53 (d, $J = 8.5$ Hz, 1H), 4.93 (s, 1H, 1), 4.35 (m, 2H), 4.15 (m, 1H), 3.8 (m, 1H), 3.6–3.2 (m, 3H), 3.1–2.6 (m, 2H), 2.6–2.3 (m, 1H), 2.3–1.8 (m, 3H), 1.05 (s, 3H, 18′).

Dyes: 4-(Dicyanomethylene)-2-methyl-6-(*p*-(bis(hydroxyethyl)amino)-styryl)-4*H*-pyran (DCMOH) was synthesized by Dr. J. Bourson according to the general procedure described in reference [40]. 3,7-Bis(diethylamino)phenoxazin-5-ium perchlorate (Ox725) was purchased from Exciton Chemical Co. and was used without further purification.

Solvent: The Britton–Robinson buffer at pH 10 (ionic strength of 0.1M) was prepared according to reference [14].

Spectroscopic measurements: All experiments were performed at 298 K. The UV/Vis absorption spectra were recorded on a Kontron Uvikon-940 spectrophotometer. Corrected fluorescence spectra were obtained with a SLM 8000 C spectrofluorometer. This apparatus was used to measure steady-state fluorescence anisotropies defined as $r = (I_\parallel - I_\perp)/(I_\parallel + 2I_\perp)$, (where $I_\parallel$ and $I_\perp$ are the fluorescence intensities observed with vertically polarized excitation light and vertically and horizontally polarized emissions, respectively).

The overall fluorescence quantum yield of CD-St was measured with 5-hydroxyquinoline in DMSO as a reference ($\Phi_F = 0.19$)[41] and found to be 0.83 ± 0.07 (the refractive index of the pH 10 buffer containing 5% of ethanol is 1.336). The fluorescence quantum yield of DCMOH in the buffer at pH 10 was determined by comparison with its known fluorescence quantum yield in DMSO (0.50)[42] and was found to be 0.073. In the presence of 7.6-fold excess of CD-St, the fluorescence enhancement is 9.9. The fluorescence quantum yield of Ox725 in the same buffer was determined by comparison with the fluorescence quantum yield of Rhodamine 101 (Exciton) in ethanol ($\Phi_F = 1$)[43] and found to be 0.052.

Time-resolved fluorescence experiments were carried out in the frequency domain. We used our multifrequency (0.1–200 MHz) phase-modulation fluorometer described elsewhere.[44] The samples were excited at 442 nm with an Omnichrome He/Cd laser. The number of frequencies used was typically 20 for double exponential decays. Phase-modulation data were analyzed by a nonlinear least-squares method with Globals software

© WILEY-VCH Verlag GmbH, D-69451 Weinheim, 1999
0947-6539/99/0512-3676 $ 17.50+.50/0 *Chem. Eur. J.* **1999**, *5*, No. 12

(Globals Unlimited, University of Illinois at Urbana-Champaign, Laboratory for Fluorescence Dynamics).

The Förster critical radius R_0 was calculated using the following equation:

$$R_0 = 0.2108\,[\kappa^2 \Phi_D n^{-4} \int_0^\infty I_D(\lambda)\varepsilon_A(\varkappa)\lambda^4 d\lambda]^{1/6} \quad (10)$$

with R_0 in Å, where κ^2 is the orientational factor, Φ_D is the quantum yield of fluorescence emission of the donor, n is the average refractive index of the medium in the wavelength range where spectral overlap is significant, $I_D(\lambda)$ is the normalized fluorescence spectrum of the donor, $\varepsilon_A(\lambda)$ is the molar absorption coefficient of the acceptor [$dm^3 mol^{-1} cm^{-1}$] and λ is the wavelength in nanometers. As already done,[6] the orientation factor was assumed to be equal to the dynamic average, that is ⅔. The refractive index was chosen to be that of tetrahydrofuran (1.407) since this solvent mimicks the interior of the CD cavity. Under these conditions, the value of R_0 calculated by Equation (10) is (34 ± 1.5) Å in the case of DCMOH and (25 ± 1.5) Å for Ox725. The standard deviation takes into account the uncertainty on the fluorescence quantum yield and on the refractive index (if $n = 1.3$ or 1.5 instead of 1.4, R_o is decreased or increased by 1 Å).

All numerical simulations have been made by using the Mathematica software.

Acknowledgment

We acknowledge Mr. Jean-Pierre Lefèvre for assistance with the lifetime measurements and Dr. Laprévote for performing the mass spectra on the CD-St samples.

[1] M. N. Berberan-Santos, J. Canceill, J. C. Brochon, L. Jullien, J. M. Lehn, J. Pouget, P. Tauc, B. Valeur, *J. Am. Chem. Soc.* **1992**, *114*, 6427–6436.
[2] M. N. Berberan-Santos, J. Pouget, B. Valeur, J. Canceill, L. Jullien, J.-M. Lehn, *J. Phys. Chem.* **1993**, *97*, 11376–11379.
[3] D. M. J. Gravett, J. Guillet, *J. Am. Chem. Soc.* **1993**, *115*, 5970–5974.
[4] L. Jullien, J. Canceill, B. Valeur, E. Bardez, J.-M. Lehn, *Angew. Chem.* **1994**, *106*, 2582–2584; *Angew. Chem. Int. Ed. Engl.* **1994**, *33*, 2438–2439.
[5] M. N. Berberan-Santos, J. Canceill, G. Gratton, L Jullien, J.-M. Lehn, P. Peter So, J. Sutin, B. Valeur, *J. Phys. Chem.* **1996**, *100*, 15–20.
[6] L. Jullien, J. Canceill, B. Valeur, E. Bardez, J.-P. Lefèvre, J.-M. Lehn, V. Marchi-Artzner, R. Pansu, *J. Am. Chem. Soc.* **1996**, *118*, 5432–5442.
[7] P. Wang, L. Jullien, B. Valeur, J.-S. Filhol, J. Canceill, J.-M. Lehn, *New J. Chem.* **1996**, *20*, 895–907.
[8] M. Nowakowska, N. Loukine, D. M. Gravett, N. A. D. Burke, J. E. Guillet, *J. Am. Chem. Soc.* **1997**, *119*, 4364–4368.
[9] P. Choppinet, L. Jullien, B. Valeur, *J. Chem. Soc. Perkin Trans. 2* **1999**, in press.
[10] M. N. Berberan-Santos, P. Choppinet, A. Fedorov, L. Jullien, B. Valeur, *J. Am. Chem. Soc.* **1999**, *121*, 2526–2533.
[11] a) G. Mc Dermott, S. M. Prince, A. A. Freer, A. M. Hawthornthwaite-Lawless, M. Z. Papiz, R. J. Cogdell, N. W. Isaacs, *Nature* **1995**, *374*, 517–521; b) X. Hu, K. Schulten, *Physics Today* **1997** (August), 28–34; c) R. Van Grondelle, R. Monshouwer, L. Valkunas, *Ber. Bunsenges. Phys. Chem.* **1996**, *100*, 1950–1957; d) T. Pullerits, V. Sundström, *Acc. Chem. Res.* **1996**, *29*, 381–389.
[12] a) H. H. Baer, Y. Shen, F. S. Gonzalez, A. V. Berenguel, J. I. Garcia, *Carbohydr. Res.* **1992**, *235*, 129–139; b) F. Guillo, B. Hamelin, L. Jullien, J. Canceill, J.-M. Lehn, L. De Robertis, H. Driguez, *Bull. Soc. Chim. Fr.* **1995**, *132*, 857–866.
[13] S. K. Chang, I. Cho, *J. Chem. Soc. Perkin Trans. 1*, **1986**, 211–214.
[14] C. Frugoni, *Gazz. Chim. Ital.* **1957**, *87*, 403–407.
[15] T. Förster, in *Modern Quantum Chemistry, Part III* (Ed. O. Sinanoglu), p. 93–137, Academic Press, New York, **1965**.
[16] a) L. Antropov, in *Electrochimie théorique*, Mir Ed, Moscow, **1979**; b) J. O'M. Bockris, A. K. N. Reddy, in *Modern Electrochemistry*, Plenum, 6th ed., New York, **1977**.
[17] In the present case, the difference of the apparent pK_a between the two carboxylic groups of MOD-St essentially originates from the repulsive electrostatic interaction between both ionized carboxylate in the doubly charged form. See note [18].
[18] This point can be appreciated by evaluating the reasonable orders of magnitude for the 14 successive pK_a of CD-St. In fact, as a result of the low available amount of CD-St, no direct experimental determination has been made. The method for deriving the successive pK_a has been described elsewhere[34] and is briefly recalled. One considers CD-St as a distribution of identical ionizable acidobasic groups (intrisic $pK_a = pK^0_{int}$) immersed in a continous medium (dielectric constant ε_r). The difference between the 14 pK_a values results from i) the additional charging work that is required to ionize an increasing number of acidobasic groups; ii) a statistical correction arising from the different numbers of proton permutations for each ionized state. For the present purpose, CD-St can be reasonably described as two aligned and parallel circular distributions of seven regularly spaced carboxylic groups. If r and a denote the radius of the charge distributions and the distance between the two distributions, respectively, one has:

$$pK_a(x) - \frac{\ln\left(\frac{x}{8-x}\right)}{\ln 10} = pK^0_{int} - \frac{N_A e^2 G_7}{8\pi\varepsilon_0\varepsilon_r RT \ln 10 r} + \frac{N_A e^2 G_7}{4\pi\varepsilon_0\varepsilon_r RT \ln 10 r}(x)$$

$x \in [1;7]$

$$pK_a(x) - \frac{\ln\left(\frac{x-7}{15-x}\right)}{\ln 10} = pK^0_{int} - \frac{N_A e^2 G_7}{8\pi\varepsilon_0\varepsilon_r RT \ln 10 r} + \frac{N_A e^2}{4\pi\varepsilon_0\varepsilon_r RT \ln 10 r}\left[\frac{G_7}{r} + \frac{H_{77}}{a}\right](x)$$

$x \in [8;14]$

G_7 and H_{77} are numerical constants that depend on r, a, the inverse Debye length κ^{-1}, the symmetry of the distribution (heptagonal in the present case). If one takes $pK^0_{int} = 5$, $r \simeq 1$ nm for the cyclodextrin radius (see ref. [32]), $a = 0.4$ nm (distance between the two carboxylic groups borne by each individual steroid unit, $\kappa^{-1} = 1$ nm (that corresponds to an ionic strength = 0.1M for a solution of monovalent salts) and $\varepsilon_r \approx 50$, one finds that the 14 values for the successive pK_a are about between 4 and 10. At pH 6 the total charge is then about 4.5 whereas it is about 13.5 at pH 10.
[19] B. Hamelin, L. Jullien, *J. Chem. Soc. Faraday Trans.* **1997**, *93*, 2153–2160.
[20] a) T. M. Stein, S. H. Gellman, *J. Am. Chem. Soc.* **1992**, *114*, 3943–3950; b) D. T. McQuade, D. G. Barrett, J. M. Desper, R. K. Hayashi, S. H. Gellman, *J. Am. Chem. Soc.* **1995**, *117*, 4862–4869; c) Y. Cheng, D. M. Ho, C. R. Gottlieb, D. Kahne, M. A. Bruck, *J. Am. Chem. Soc.* **1992**, *114*, 7319–7320; d) P. Venkatesan, Y. Cheng, D. Kahne, *J. Am. Chem. Soc.* **1994**, *116*, 6955–6956; e) C. J. Burrows, R. A. Saute, *J. Inclusion Phenom.* **1987**, *5*, 117–121; f) V. Janout, M. Lanier, S. L. Regen, *J. Am. Chem. Soc.* **1996**, *118*, 1573–1574; g) B. Hamelin, L. Jullien, A. Laschewsky, C. Hervé du Penhoat, *Chem. Eur. J.* **1999**, *5*, 546–556.
[21] Ox725 has been already used as a guest for complexation by the native β-cyclodextrin, see: W. G. Herkstroeter, P. A. Martic, S. Farid, *J. Am. Chem. Soc.* **1990**, *112*, 3583–3589.
[22] At larger concentrations, the inner-filter effects appear.
[23] G. S. Levinson, W. T. Simpson, W. Curtis, *J. Am. Chem. Soc.* **1957**, *79*, 4314–4320.
[24] By expressing the equilibrium constant associated to the Equation (1) assuming that activities and concentrations are identical and by writing the conservation law for DCMOH, the concentration in free DCMOH [DCMOH], and in its dimeric form [$(DCMOH)_2$] are expressed as a function of $[DCMOH]_{tot}$. These expressions are then introduced in Eq. (2a) to yield Eq. (2b).
[25] The method for correcting the contribution of direct excitation has been reported in a previous paper, see ref. [6].
[26] W. Likussar, D. F. Boltz, *Anal. Chem.* **1971**, *43*, 1265–1272.
[27] L. Jullien, B. Valeur, unpublished results.
[28] Y. Inoue, T. Hakushi, Y. Liu, L. H. Tong, B. J. Shen, D. S. Jin, *J. Am. Chem. Soc.* **1993**, *115*, 475–481, and references therein.
[29] C. R. Cantor, P. R. Schimmel, *Biophysical Chemistry*, *Part II*, Freeman, New York, **1980**.

[30] The DCMOH orientation within the CD-NA cavity was analyzed by circular dichroism by using established correlations between the guest orientation and the shape of the CD signal, see ref. 6. In view of the intrinsic chirality of the steroid walls, it was impossible to use the same methodology in the CD-St case.
[31] T. Tao, *Biopolymers* **1972**, *8*, 609 – 632.
[32] a) J. Perrin, *J. Phys. Radium*, **1934**, *5*, 497 – 511; b) J. Perrin, *J. Phys. Radium* **1936**, *7*, 1 – 11.
[33] B. Hamelin, L. Jullien, C. Derouet, C. Hervé du Penhoat, P. Berthault, *J. Am. Chem. Soc.* **1998**, *120*, 8438 – 8447.
[34] L. Jullien, H. Cottet, B. Hamelin, A. Jardy, *J. Phys. Chem.* in press.
[35] According to the method that is developed in ref. [34], the standard Gibbs free energy of association between the seven times identically charged CD-NA units can be written:

$$\Delta_r G^0_{77} = \frac{e^2 N_A 7^2}{4\pi\varepsilon_0\varepsilon_r d} H_{77}$$

where d denotes the distance between the centers of the parallel circular distributions of the CD-NA charges and by keeping the notations introduced in note [18]. By taking $d = 3$ nm to derive a reasonable estimate in view of the hydrodynamic description that was extracted from the steady-state emission anisotropy of DCMOH, one finds $\Delta_r G^0_{77} \approx 15\ \mathrm{kJ\,mol^{-1}}$ at $\kappa^{-1} = 1$ nm ($H_{77} = 0.33$ at 0.1 M ionic strength) and $\Delta_r G^0_{77} \approx 30\ \mathrm{kJ\,mol^{-1}}$ at $\kappa^{-1} = 4$ nm ($H_{77} = 0.70$ at 0.005 M ionic strength).
[36] I. Rouzina, V. A. Bloomfield, *J. Phys. Chem.* **1996**, *100*, 4292 – 4304; I. Rouzina, V. A. Bloomfield, *J. Phys. Chem.* **1996**, *100*, 4305 – 4313; U. Mohanty, B. W. Ninham, I. Oppenheim, *Proc. Natl. Acad. Sci. USA* **1996**, *93*, 4342 – 4344.
[37] Such a point was already discussed in another cyclodextrin series, see: B. Hamelin, L. Jullien, F. Guillo, J.-M. Lehn, A. Jardy, L. De Robertis, H. Driguez *J. Phys. Chem.* **1995**, *99*, 17877 – 17885. A first insight can be obtained by using the criterium that was originally introduced by Manning (G. S. Manning, *Q. Rev. Biophys.* **1978**, *11*, 179 – 246) for determining whether one is in a regime of counterion condensation or not for a rod-like polyelectrolyte. Manning introduces ξ as the ratio between the Bjerrum length l_B ($e^2/4\pi\varepsilon_r\varepsilon_0 kT$) to spacing b between the charges borne by the linear polyelectrolyte. ε_r is the dielectric constant, k the Boltzmann's constant and e the electronic charge. If the buffer contains only monovalent counterions (cations in the present case), one would observe the counterion condensation when $\xi > \xi_{crit} = 1$. If one assimilates both CD-NA and CD-St cyclodextrins as rings (radius $\simeq 1$ nm) of regularly spaced elementary charges (7 for CD-NA and 14 for CD-St at pH 10; vide supra), one finds $\xi = 0.8$ for CD-NA whereas $\xi = 1.6$ for CD-St.
[38] W. E. Bachmann, A. Dreiding, *J. Am. Chem. Soc.* **1950**, *72*, 1323 – 1329.
[39] If the mixture was not treated with 1 M NaOH, a mixture of two carboxylic acids was obtained: m.p. 226 °C and 245 – 250 °C. They can be easily separated by crystallization in CH_2Cl_2 or CH_3OH. The compound melting at 245 – 250 °C was identified as the bisdehydromarrianolic acid from its melting point already reported in the literature (J. Heer, J. R. Billeter, K. Miescher, *Helv. Chim. Acta* **1945**, *28*, 991 – 1003). It can be converted into the compound melting at 226 °C by dissolution in 1 M NaOH.
[40] J. Bourson, B. Valeur, *J. Phys. Chem.* **1989**, *93*, 3871 – 3876.
[41] M. Goldman, E. L. Wehry, *Anal. Chem.* **1970**, *42*, 1178 – 1178.
[42] X. Armand, J. Bourson, unpublished results.
[43] D. F. Eaton, *Pure Appl. Chem.* **1988**, *60*, 1107 – 1114.
[44] J. Pouget, J. Mugnier, B. Valeur, *J. Phys. E Sci. Instr.* **1989**, *22*, 855 – 862.

Received: March 22, 1999 [F 1691]

 © WILEY-VCH Verlag GmbH, D-69451 Weinheim, 1999 0947-6539/99/0512-3678 $ 17.50+.50/0